

# Fault detection and isolation of sensors in aeration control systems – the airflow ratio method

Bengt Carlsson and Jesús Zambrano

Division of System and Control, Department of Information Technology, Uppsala University, P.O. Box 337, SE-75105 Uppsala, Sweden.

(E-mail: [bengt.carlsson@it.uu.se](mailto:bengt.carlsson@it.uu.se), [jesus.zambrano@it.uu.se](mailto:jesus.zambrano@it.uu.se)).

**Abstract:** In this paper, we consider the problem of detecting sensor faults in the aeration system of an activated sludge process. The purpose is to detect possible faults in the dissolved oxygen sensors. The dissolved oxygen concentration in each aerated zone is assumed to be automatically controlled. As the basis for a fault detection algorithm we propose to use the ratio of air flow rates into different zones. The method is evaluated by using the Benchmark Simulation Model n°1 (BSM1) via Monte Carlo simulations. Results show that this method gives a good performance in terms of a correct and early fault detection and isolation.

**Keywords:** Aeration control; fault detection; isolation; monitoring; incidence matrix.

## INTRODUCTION

Fault detection and isolation is an active area of research due to increasing complexity of industrial processes and growing demand for safety and reliability. In general, given an industrial process with multiple sensors and actuators, fault detection techniques applied to this process will depend on if the aim is to detect faults from single or multiple variables. The variables can be signals from sensors and/or actuators.

Several fault detection techniques have been developed in wastewater treatment plants, considering the monitoring of aeration in a single zone (Corominas et al., 2011), as well as the monitoring of other process variables like flow rate, pH, ammonia, temperature (Rosen and Lennox, 2001; Choi and Lee, 2004; Baggiani and Marsili-Libelli, 2009). Steyer et al. (2001) study two kinds of faults in an anaerobic digestion processes: abrupt and incipient (e.g. drift changes). The first type occurs when the process state changes quickly and is in general easier to detect than the second type.

In Corominas et al. (2011), the sensor fault detection in systems under feedback control was studied. This problem poses special challenges, since if a sensor signal is used in a feedback control law, a fault in the sensor may not be visible from the sensor signal itself because the controller strive to keep (the possible faulty) sensor signal equal to the set point.

In this paper, the problem to detect sensor faults in the aeration system of an activated sludge process (ASP) is considered, in particular faults in dissolved oxygen (DO) sensors under closed loop control. Therefore, the case study consists of fault detection in a process with a number of aerated zones, assuming that the DO concentration in each zone is automatically controlled by adjusting the airflow rate.

As the basis for the fault detection algorithm we propose to monitor the ratio of airflow rates into different zones. The reason is that these ratios are less dependent on the influent load compared to using the individual airflow rates separately. The behavior of the ratios for different fault locations allows the development of an incidence matrix which is used to get the isolation of the fault.

The paper is organized as follows. First, two methods for detecting faults in DO sensors are outlined. Next, a set of evaluation indexes are defined and a simulation protocol is outlined. Then, a case study using the BSM1 is presented and the results from the methods are shown. Finally, the results are discussed and conclusions are drawn.

## METHOD

An ASP with  $N$  aerated zones in series is considered. The DO in each zone is in closed loop control by individual adjustments of the air flow rate into each zone. It is assumed that the air flow rate is measured and a possible fault occurs in one of the DO sensors. Just one fault per zone at a time is considered in this study. If also faults may occur in the air flow rate sensors it will not be possible to distinguish those faults from the faults in the DO sensor and we will then only have the possibility to decide in which zone there is a sensor (DO or air flow rate) fault.

### The Airflow Method (AM)

A very simple method to detect a faulty DO sensor is by monitoring the airflow rate in every zone. In this method, a sensor fault in zone  $i$  is decided if:

$$\bar{q}_i(t) < a_i \text{ or } \bar{q}_i(t) > b_i \quad (1)$$

where  $a_i$  and  $b_i$  are the minimum and maximum bounds respectively, defined as:

$$a_i = \alpha_{min} \cdot \min \{ \bar{q}_i(t) |_{t \in A} \} \quad ; \quad b_i = \alpha_{max} \cdot \max \{ \bar{q}_i(t) |_{t \in A} \} \quad (2)$$

where:

$\bar{q}_i(t)$  is a low-pass filtered value of the airflow rate into zone  $i$ .

$\alpha_{min}$  and  $\alpha_{max}$  are threshold factors used to define the lower and upper bounds, respectively.

$A$  is a set of data in non-faulty conditions.

### The Airflow Ratio Method (ARM)

A slightly more sophisticated approach is to monitor the *ratio* of the airflow rates between the zones. ARM calculates maximum values on airflow rate ratios between zones during normal (non-faulty) conditions, and uses these values as bounds for detecting a fault. In this method, a sensor fault is decided if:

$$f_{i,j}(t) > \gamma_{i,j} \quad ; \quad \text{for } i = 1, 2, \dots, N; \quad j = 1, 2, \dots, N \quad (i \neq j) \quad (3)$$

where:

$$f_{i,j}(t) = \bar{q}_i(t)/\bar{q}_j(t).$$

$\bar{q}_i(t)$  is a low-pass filtered value of the airflow rate into zone  $i$ .

$\gamma_{i,j} = \alpha_{i,j} \cdot f_{i,j}^{max}$ , is the threshold value.

$\alpha_{i,j}$  is a threshold factor.

$$f_{i,j}^{max} = \max \left\{ \bar{q}_i(t)/\bar{q}_j(t) \Big|_{t \in A} \right\}.$$

$A$  is a set of data in non-faulty conditions.

Given  $N$  zones, there are  $N(N-1)$  airflow ratios  $f_{i,j}(t)$ . Therefore, a fault is decided if any of these ratios is above its threshold value.

### Fault isolation

Since AM is based on the signal monitoring in every zone, the fault isolation in zone  $i$  is decided when a sensor fault in zone  $i$  is decided.

For ARM, the method to decide a fault isolation in zone  $i$  has to be different since the decision for a fault detection is based on the ratio of variables. For example, consider the response of ARM for the case of a negative bias in the DO sensor of zone  $i$ . In this case the airflow rate in this zone will tend to increase, then all the  $f_{i,j}$  ratios are likely to be greater than  $f_{i,j}^{max}$ . On the other hand, if the fault is a positive bias in the DO sensor of zone  $j$ , the airflow rate in this zone will tend to decrease, then all the  $f_{i,j}$  ratios are likely to be greater than  $f_{i,j}^{max}$ . Therefore, different faults correspond to different ratio responds.

A basic way to classify these results is by using binary evaluation of every airflow ratio against the thresholds (Gertler, 1998). This structure gives an *observed fault signature*  $\varphi_{i,j}$ . Applications of the observed fault signature can be found in Fagarasan and Iliescu (2008), used as a tool to isolate the fault source. Making use of this structure we get:

For a negative bias in the DO sensor of zone  $i$ :

$$\varphi_{i,j}(t) = \begin{cases} 1 & \text{if } f_{i,j}(t) > \gamma_{i,j} \\ 0 & \text{otherwise} \end{cases} \quad \text{for } i = 1, \dots, N; j = 1, \dots, N \ (i \neq j) \quad (4)$$

For a positive bias in the DO sensor of zone  $j$ :

$$\varphi_{i,j}(t) = \begin{cases} 1 & \text{if } f_{i,j}(t) > \gamma_{i,j} \\ 0 & \text{otherwise} \end{cases} \quad \text{for } i = 1, \dots, N; j = 1, \dots, N \ (i \neq j) \quad (5)$$

These observed fault signatures allows isolation of a faulty DO sensor. The observed fault signature for every scenario can be ordered in an *incidence matrix*. Regarding biological processes, the incidence matrix has previously been used for isolation of multiple actuator and sensor faults in a waste water treatment process (Fragkoulis et al., 2011), as part of a methodology for fault measurement detection in a urban water supply

network (Ragot and Maquin, 2006), and as part of a fault diagnosis algorithm applied to sewer networks (Meseguer et al., 2010). Table 1 shows the incidence matrix for the case of  $N=3$  (i.e., 3 zones in series).

**Table 1.** Incidence matrix for 3 zones in series

	$\varphi_{1,2}$	$\varphi_{1,3}$	$\varphi_{2,1}$	$\varphi_{2,3}$	$\varphi_{3,1}$	$\varphi_{3,2}$
negative bias in DO1	1	1	0	0	0	0
negative bias in DO2	0	0	1	1	0	0
negative bias in DO3	0	0	0	0	1	1
positive bias in DO1	0	0	1	0	1	0
positive bias in DO2	1	0	0	0	0	1
positive bias in DO3	0	1	0	1	0	0

### Index for evaluation of fault detection performance

Based on the observed fault signature described previously, a set of indexes are proposed in order to evaluate and compare the performance of the different fault detection methods in terms of detection and isolation. These indexes are calculated considering the time of the fault occurrence, the time of fault detection and the time of fault isolation, see Figure 1.

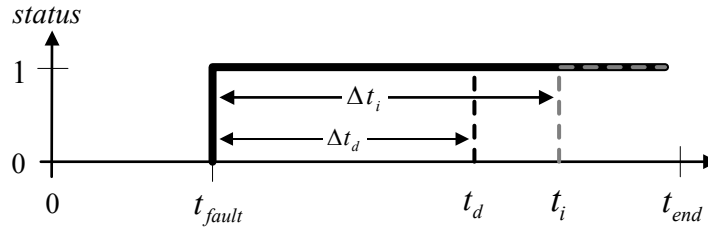


**Figure 1.** True sensor status (black line), the time when a fault is detected (dashed black) and the time for isolation (dashed gray).

In figure 1,  $t_{fault}$ ,  $t_d$  and  $t_i$  are the time of the fault occurrence, the time of the fault detection and the time of the fault isolation, respectively.  $\Delta t_d$  and  $\Delta t_i$  are the times needed for the fault detection ( $\Delta t_d = t_d - t_{fault}$ ) and fault isolation ( $\Delta t_i = t_i - t_{fault}$ ), respectively.  $t_{end}$  is the total evaluation time. The sensor status is represented by a binary variable where the values 0 and 1 refer to non-faulty and faulty sensor, respectively.

In order to evaluate the performance of the algorithms in terms of the *percentage* of fault detections, false identifications, and false alarms, the following indexes are used:

$$FD = \left( \frac{1}{M} \sum_{k=1}^M n_{FD}^{[k]} \right) \cdot 100 \quad \text{where: } n_{FD}^{[k]} = \begin{cases} 1 & \text{if } t_{fault} < t_d < t_{end} \\ 0 & \text{otherwise} \end{cases} \quad (6)$$

$$FI = \left( \frac{1}{M} \sum_{k=1}^M n_{FI}^{[k]} \right) \cdot 100 \quad \text{where: } n_{FI}^{[k]} = \begin{cases} 1 & \text{if } t_d < t_i < t_{end} \\ 0 & \text{otherwise} \end{cases} \quad (7)$$

$$FA = \left( \frac{1}{M} \sum_{k=1}^M n_{FA}^{[k]} \right) \cdot 100 \quad \text{where: } n_{FA}^{[k]} = \begin{cases} 1 & \text{if } t_d < t_{fault} \\ 0 & \text{otherwise} \end{cases} \quad (8)$$

where  $FD$  is the percentage of fault detections;  $FI$  is the percentage of fault isolations and  $FA$  is the percentage of false alarms.  $M$  refers to the total number of simulation runs, and  $k$  refers to the  $k^{th}$  simulation.

For AM the time of the fault detection and the time of the fault isolation are the same ( $t_d = t_i$ ). When ARM is used, the decision of fault detection and fault isolation are made separately. Therefore, in order to take into account the time involved in the fault detections and isolations, a fault detection index ( $I_{FD}$ ) and fault isolation index ( $I_{FI}$ ) have been defined as follows:

$$I_{FD} = \left( 1 - \frac{1}{M \cdot t_{end}} \sum_{k=1}^M t_{FD}^{[k]} \right) \cdot 100 \quad (9)$$

where:  $t_{FD}^{[k]} = \begin{cases} \Delta t_d & \text{for a correct fault detection} \\ t_{end} & \text{otherwise} \end{cases}$

$$I_{FI} = \left( 1 - \frac{1}{M} \sum_{k=1}^M \frac{t_{FI}^{[k]}}{(t_{end} - t_{fault})} \right) \cdot 100 \quad (10)$$

where:  $t_{FI}^{[k]} = \begin{cases} \Delta t_i & \text{for a correct fault isolation} \\ t_{end} - t_{fault} & \text{otherwise} \end{cases}$

Given a correct fault detection ( $t_{fault} < t_d < t_{end}$ ), a value of  $I_{FD}$  close to 100 is given when  $t_{FD}$  is close to 0 (this is,  $t_d$  is close to  $t_{fault}$ ), indicating a short time delay in the fault detection. Similarly, given a correct fault isolation ( $t_d < t_i < t_{end}$ ), a value of  $I_{FI}$  close to 100 is given when  $t_{FI}$  is close to 0 (this is,  $t_i$  is close to  $t_d$ ), indicating a short time delay in the fault isolation. Therefore, values of  $I_{FD}$  and  $I_{FI}$  close to 100 indicate a good performance in terms of fault detection and fault isolation, respectively.

### CASE STUDY: 3 Zones in BSM1

The BSM1 (Copp, 2002) was selected as the simulation platform. The BSM1 includes model, plant layout (pre-denitrification plant with five activated sludge zones in series, two anoxic and three aerobic), control systems and a benchmark procedure. The system was simulated using the MATLAB/Simulink® platform.

Three different dynamic influents were considered: dry, rain and storm. The simulation time was extended from 14 to 21 days in order have some more days for the fault detection evaluations. The DO feedback PI-control in zone 5 was also applied to zone 3 and 4 (see Figure 2). Every control loop has a set-point of 2 mgO<sub>2</sub>/l. The nitrate feedback PI-controller in the second anoxic compartment is kept as by default. We use the notation DO<sub>j</sub> for the DO sensor in zone  $j$ .

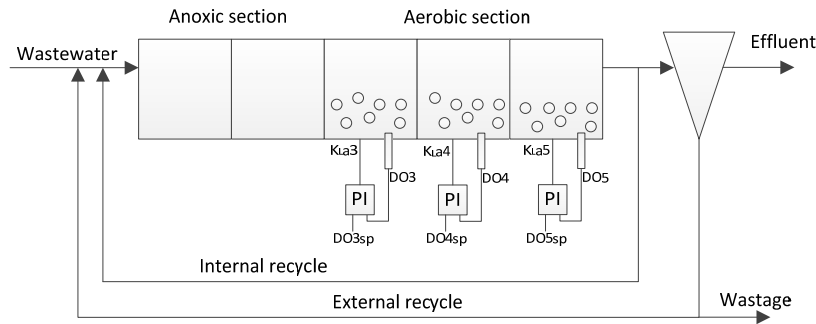


**Figure 2.** Case study

### Sensor modeling

The sensor models are based on the study given by Rieger et al. (2003). The DO sensors belong to class A, and have a response time of 1 min in non-faulty conditions, a measurement range of 0–10 mgO<sub>2</sub>/l and a noise standard deviation of 0.25 mgO<sub>2</sub>/l. Details of the sensor model can be found in Rosen et al. (2008) and Corominas et al. (2010).

### Fault modeling

The implementation of the faults was assessed based on the approach developed by Corominas et al. (2011) and previous work given by Rosen et al. (2008). Here, fault vectors with five elements ( $v_1, \dots, v_5$ ) are defined for the different type of faults. Table 2 shows the fault vector related to different sensor statuses. These elements add and/or multiply certain values to the true value in order to model the correspondent sensor status. The parameters of the fault implementations are  $f_b$  (bias),  $f_g$  (doubling of the slope of calibration curve),  $f_r$  (drift speed) and  $c_0$  (calibration speed).

**Table 2.** Vector used to describe different faults (taken from Corominas et al. 2010)

Sensor status	Fault vector				
	$v_1$	$v_2$	$v_3$	$v_4$	$v_5$
1. Fully functional	[1	0	0	1	0]
2. Shift	[1	$f_b$	0	1	0]
3. Excessive drift	[1	$-(t-t_0)f_r$	0	1	0]
4. Fixed value	[0	0	0	0	1]
5. Complete failure	[0	0	0	1	0]
6. Wrong gain	[ $f_g$	0	$(1-f_g) \cdot c_0$	1	0]
7. Calibration	[0	0	0	0	1]

This study will focus on bias errors and new noise levels in the DO sensor. Regarding the bias, this type of fault is named as “shift” in Table 2. Therefore a bias is added via the  $f_b$  parameter. In this study,  $f_b$  has a range of 0–1 mg/l. About the noise fault, a new noise level is added to the sensor model, because this type of fault is not defined in Table 2.

### Simulation Protocol

The protocol to evaluate the performance of AM and ARM is described as follows:

- Step 1: A number of dynamic simulations are executed for different influent events (dry, rain and storm) in non-faulty conditions. Here, the thresholds for AM and ARM algorithms are calculated.
- Step 2: An influent event (dry, rain or storm) and a faulty DO sensor (zone 3, 4 or 5) are selected.
- Step 3: BSM1 is simulated for 150 days in order to reach steady state conditions.
- Step 4: A dynamic simulation is performed during 21 days. Here, the time of the fault event ( $t_{fault}$  in Figure 1) is generated via Monte Carlo method. This is, the domain of the possible fault time is defined (in this case, the fault may occur between day 7 and 14); then, the fault time is generated randomly from a probability distribution over the domain. The performance indexes are calculated during the 21 days in order to also detect false alarms.
- Step 5: If the  $k^{th}$  run is  $< M$  (total number of simulations), go to Step 3. Otherwise, go to Step 2.

### Simulation Scenarios

The case study is tested considering different location of the faulty sensor (in zone 3, 4 and 5); three influent conditions (dry, rain and storm); two types of faults (bias and a changed noise level), assuming that there is only one type of fault generated at a time for any scenario, and different threshold factors ( $\alpha = 1.02$  and  $1.05$ ), this is, the threshold values for AR ( $a_i ; b_i$ ) and for ARM ( $\gamma_{i,j}$ ) were calculated considering a value of  $\alpha = 1.02$  (2%) and  $\alpha = 1.05$  (5%).

Currently no air flow model is defined in BSM1. For simplicity,  $K_{La}$  was selected as the monitored variable for AM and ARM algorithms. In practice, the measurement of the air flow rate should obviously be used.

Concerning the parameters of the simulations, it was assumed a sample time of 1 minute for the  $K_{La}$ -values, and a low-pass filtered implemented by a moving average window of 15 samples. By default, the threshold values for AR ( $a_i ; b_i$ ) and for ARM ( $\gamma_{i,j}$ ) were calculated with  $\alpha = 1.05$ . The total number of simulations (see  $M$  value in previous section) for every influent event and faulty simulations is  $M = 20$ .

## RESULTS

### Illustrative example

We will first illustrate the method when a positive bias of  $1\text{mgO}_2/\text{l}$  is applied to the DO sensor in zone 5 (DO5). Figure 3 shows the airflow ratio profiles in non-faulty and faulty conditions.

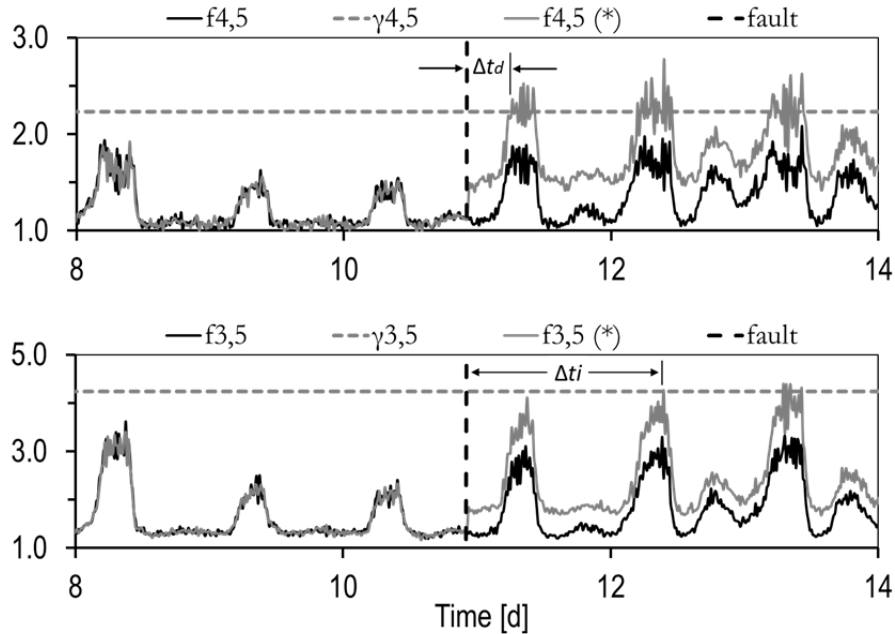


**Figure 3.** Airflow ratio response in normal conditions ( $f_{i,j}$  in black), and when a bias of  $1\text{mgO}_2/\text{l}$  is applied in DO5 ( $f_{i,j}^*$ , in gray). The thresholds (in dashed gray) and the fault occurrence (in dashed black) are shown.

In this particular example, the positive bias fault in DO5 happens at 10.92d. Using the incidence matrix given in Table 1, the *observed fault signature* for this scenario is showed in Table 3.

**Table 3.** Observed fault signature for a positive bias in DO5

	$\varphi_{3,4}$	$\varphi_{3,5}$	$\varphi_{4,3}$	$\varphi_{4,5}$	$\varphi_{5,3}$	$\varphi_{5,5}$
positive bias in DO5	0	1	0	1	0	0

It can be observed in Figure 3 that  $f_{4,5}$  is the first ratio above the threshold, yielding  $\varphi_{4,5} = 1$ , therefore a sensor fault is decided. The second ratio above the threshold is  $f_{3,5}$ , giving  $\varphi_{3,5} = 1$ . Hence, a fault in DO5 is decided. Furthermore, note the delay in the fault detection ( $\Delta t_d$ ) and the delay in the fault isolation ( $\Delta t_i$ ).



### Detection of bias faults

Detection of faults due to a bias in the DO sensors was studied. Table 4 summarizes the results of the index evaluation for AM and ARM when a bias of 1 mgO<sub>2</sub>/l is applied. The evaluation considers different influent conditions (dry, rain and storm), and location of the fault sensor (zone 3, 4 and 5).

**Table 4.** Index results for detection of bias faults

Inf.	Zone	Method	$\Delta t_d$ [d]	$\Delta t_i$ [d]	FD [%]	FI [%]	FA [%]	I <sub>FD</sub> [%]	I <sub>FI</sub> [%]
Dry	3	AM	1.75 +/- 1.67		100	100	0	91.7	83.4
		ARM	0.03 +/- 0.03	0.18 +/- 0.17	100	100	0	99.9	98.3
	4	AM	0.54 +/- 0.52		100	100	0	97.5	94.9
		ARM	0.07 +/- 0.09	0.46 +/- 0.24	100	100	0	99.7	95.6
	5	AM	0.61 +/- 0.81		100	100	0	97.1	94.2
		ARM	0.21 +/- 0.21	0.32 +/- 0.27	100	100	0	99.0	97.0
Rain	3	AM	0.59 +/- 0.45		100	100	0	97.2	94.3
		ARM	0.03 +/- 0.05	0.07 +/- 0.1	100	100	0	99.9	99.3
	4	AM	0.82 +/- 0.81		90	100	10	93.3	85.4
		ARM	0.03 +/- 0.02	1.93 +/- 1.62	95	100	5	97.5	78.3
	5	AM	1.56 +/- 1.45		100	100	0	92.6	85.2
		ARM	0.62 +/- 0.77	1.55 +/- 1.45	100	100	0	97.1	85.2
Storm	3	AM	0.58 +/- 0.58		100	75	0	97.3	64.3
		ARM	0.05 +/- 0.06	0.11 +/- 0.1	100	100	0	99.8	99.0
	4	AM	0.69 +/- 0.63		100	75	0	96.7	63.4
		ARM	0.07 +/- 0.09	0.78 +/- 0.60	100	90	0	99.7	93.4
	5	AM	1.47 +/- 1.44		100	100	0	93	86.0
		ARM	0.45 +/- 0.43	1.01 +/- 0.98	100	100	0	97.9	90.4

The effect of different levels of bias was studied in order to evaluate the performance of the AM and ARM in terms of fault detections and false alarms. For that, a range in bias from +/- 0.25 to +/- 1 mgO<sub>2</sub>/l was considered. The non-faulty condition (0 mgO<sub>2</sub>/l) is also included in this evaluation. This study considered different locations of the faulty sensor (zone 3, 4 and 5); and different influent conditions (dry, rain and storm). Results of the percentage of fault detections (FD) and false alarms (FA) are shown in Figure 4.

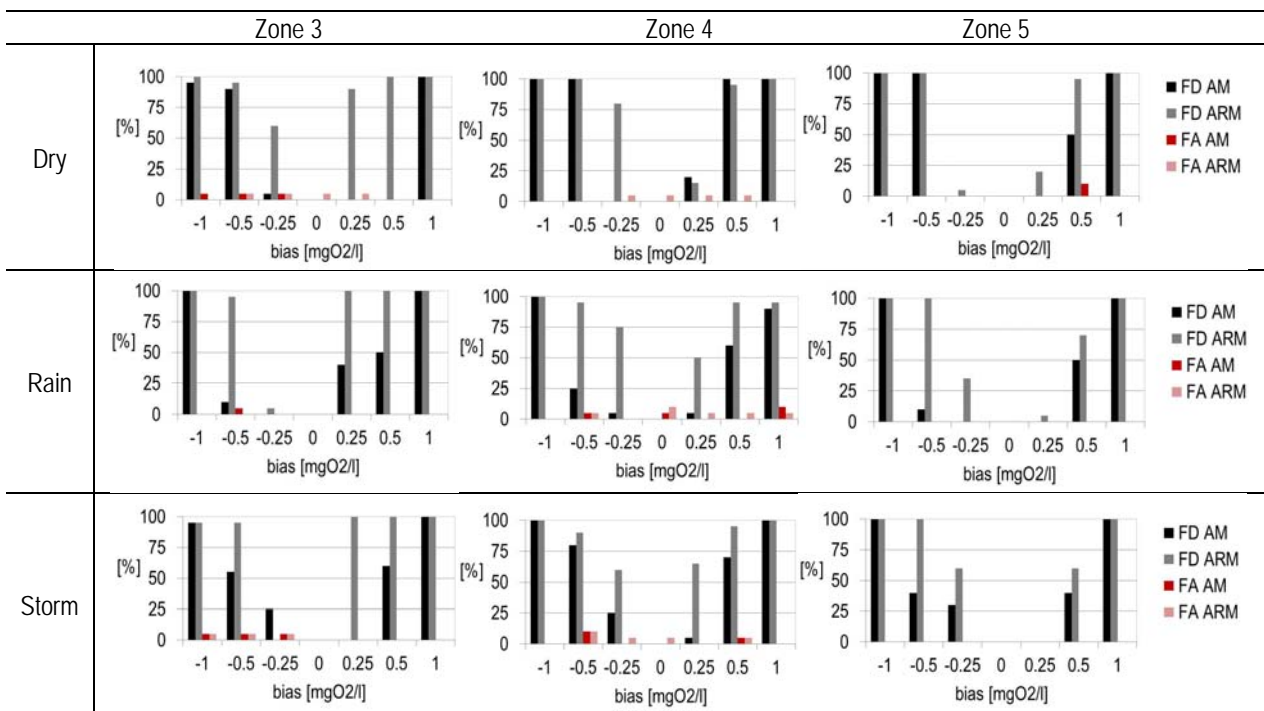


**Figure 4.** Percentage of fault detection (FD) and false alarms (FA) for AM and ARM methods considering the scenario of bias faults.

**Detection of changes in the noise level**

The effect of changes in the noise level was studied as another example of fault in the DO sensors. In this case, an increase in the noise standard deviation ( $n\sigma$ ) from its default value (0.25 mgO<sub>2</sub>/l) was used. Table 5 summarizes the results of the index evaluation for AM and ARM when the noise standard deviation is changed to 1 mgO<sub>2</sub>/l. The evaluation considers different influent conditions (dry, rain and storm), and location of the fault sensor (zone 3, 4 and 5).

**Table 5. Index results for detection of changes noise level**

Inf.	Zone	Method	$\Delta t_d$ [d]	$\Delta t_i$ [d]	FD [%]	FI [%]	FA [%]	I <sub>FD</sub> [%]	I <sub>FI</sub> [%]
Dry	3	AM	5.28 +/- 2.09		15	66.67	0	11.23	6.60
		ARM	1.19 +/- 1.09	3.11 +/- 2.08	95	84.21	5	89.59	57.91
	4	AM	1.10 +/- 1.27		100	100	0	94.72	89.46
		ARM	0.47 +/- 0.72	1.77 +/- 1.27	100	95	0	97.76	84.01
	5	AM	1.00 +/- 1.00		100	100	0	95.21	90.44
		ARM	0.43 +/- 0.31	0.71 +/- 0.59	100	100	0	97.94	93.22
Rain	3	AM	1.28 +/- 1.28		55	100	0	51.63	56.16
		ARM	0.84 +/- 0.71	2.41 +/- 2.09	100	95	0	96	74.52
	4	AM	2.47 +/- 1.85		100	100	0	88.22	76.39
		ARM	0.40 +/- 0.55	2.83 +/- 1.61	100	100	0	98.07	72.97
	5	AM	1.67 +/- 1.42		100	100	0	92.03	84.04
		ARM	0.32 +/- 0.24	0.83 +/- 0.66	100	100	0	98.47	92.05
Storm	3	AM	1.42 +/- 1.06		65	100	0	60.60	61.33
		ARM	0.84 +/- 0.70	2.11 +/- 1.64	90	94.44	10	86.38	67.60
	4	AM	1.71 +/- 1.41		100	100	0	91.81	83.64
		ARM	0.40 +/- 0.37	1.96 +/- 1.14	100	100	0	98.09	81.29
	5	AM	1.20 +/- 1.11		100	100	0	94.27	88.57
		ARM	0.46 +/- 0.44	0.84 +/- 0.72	100	100	0	97.78	91.92

Figure 5 shows the results of the percentage of fault detections (FD) and false alarms (FA) when a change in the noise standard deviation is changed from 0.25 to 0.5 and to 1 mgO<sub>2</sub>/l.

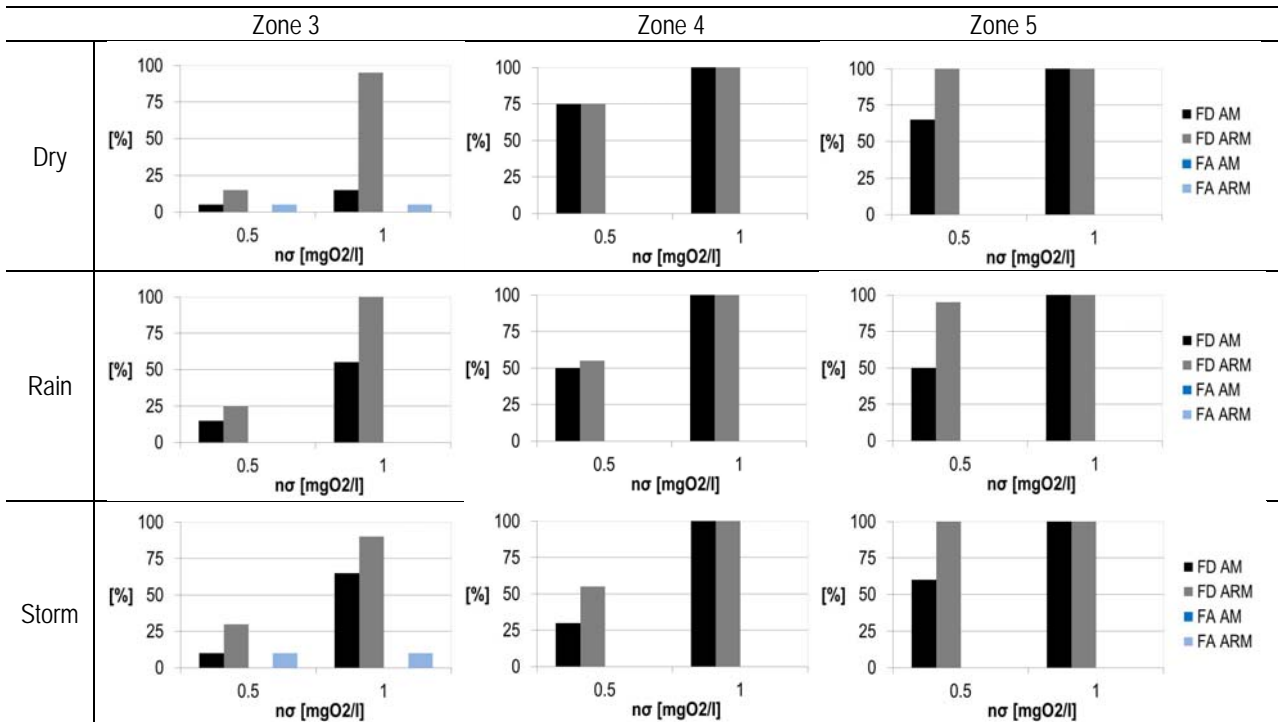


**Figure 5.** Percentage of fault detection (FD) and false alarms (FA) for the AM and ARM methods considering the scenario of change in noise level.

### Influence on the threshold parameters

The definition of the thresholds involves a compromise between fast fault detection and low false alarm frequency. A low value of the thresholds increases the sensibility to the fault detections but also increases the false alarms. On the other hand, a high value of bounds reduces the false alarms but also reduces the ability to detect faults. Therefore, changes in the threshold levels were considered in order to see its effect in the performance of the AM and ARM techniques. Two levels of thresholds were tested:  $\alpha = 1.02$  (2%) and 1.05 (5%). Figure 6 shows the influence of the threshold in the performance of AM and ARM for different levels of bias. Results are shown for the case of dry weather influent and DO3 as the faulty sensor.

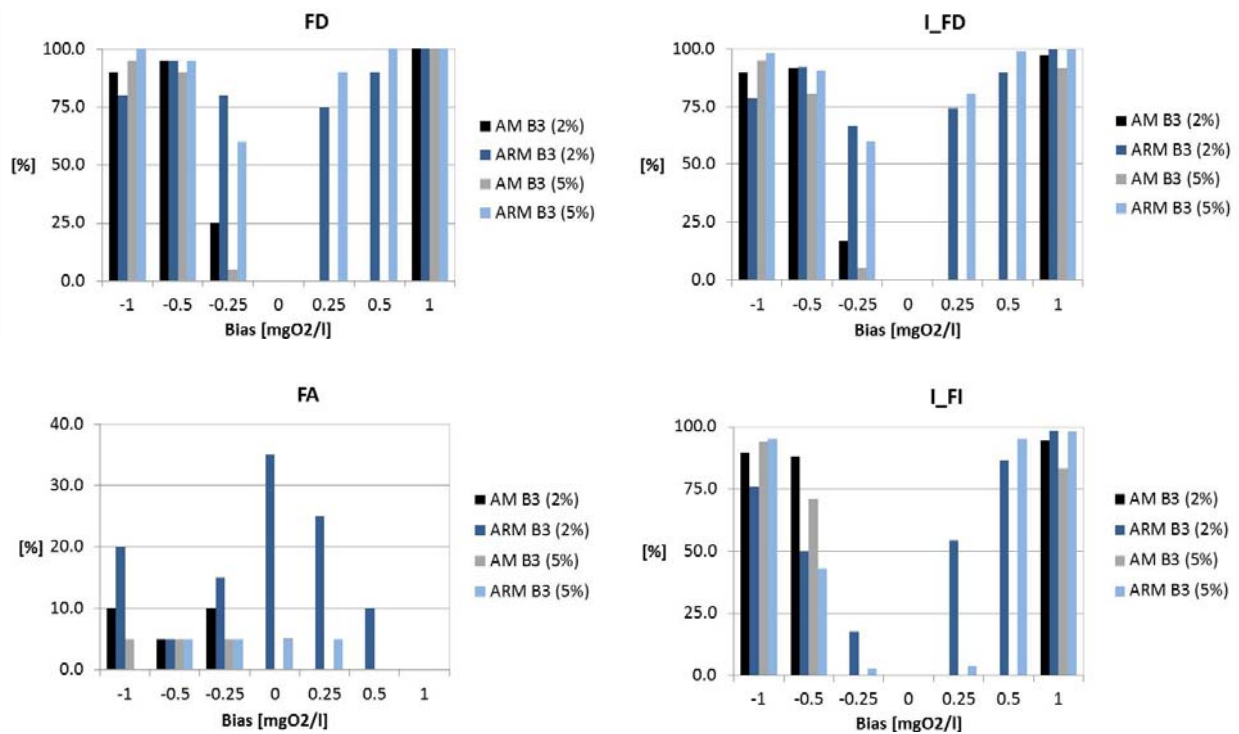


**Figure 6.** Results of AM and ARM under different bias faults (from 0 to +/- 1mgO<sub>2</sub>/l), for two thresholds ( $\alpha = 1.02$  (2%) and 1.05 (5%)). Results are shown for dry condition and DO3 as the faulty sensor.

Figure 7 shows the influence of the threshold in the performance of AM and ARM for different levels of noise. Results are shown for the case of dry weather and DO3 as the faulty sensor.

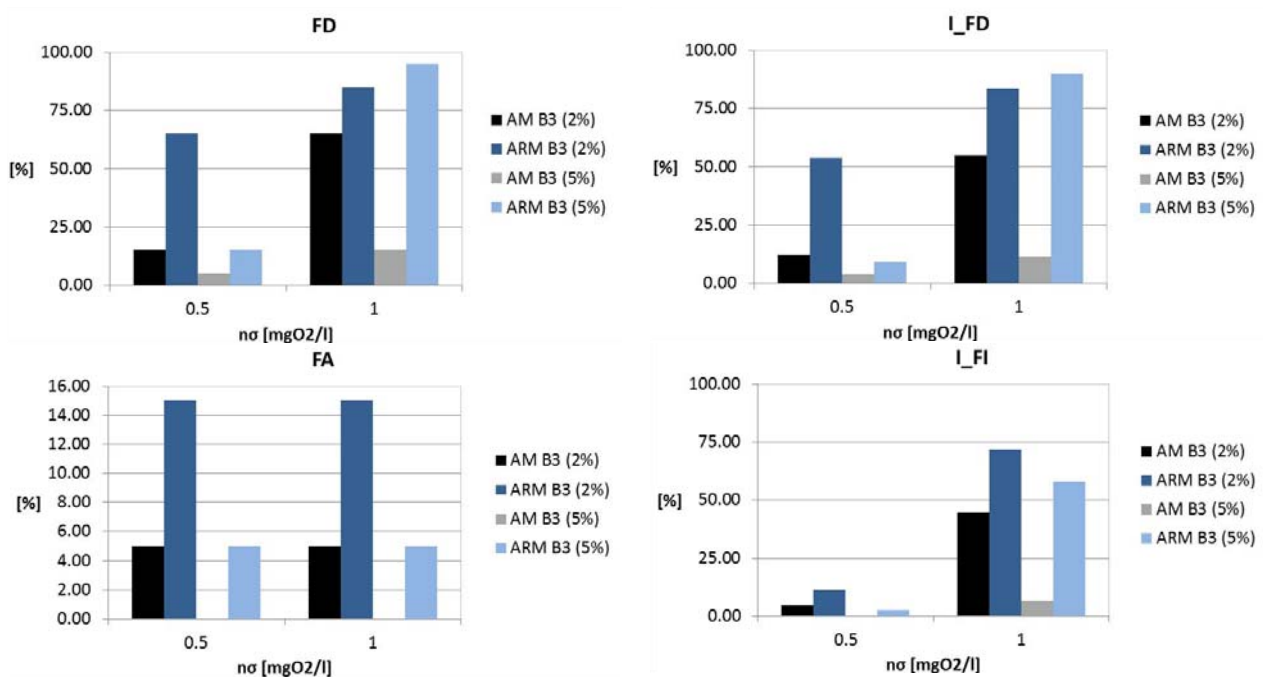


**Figure 7.** Results of AM and ARM when the standard deviation of the sensor noise is changed to 0.5 and 1 mgO<sub>2</sub>/l, for two thresholds ( $\alpha = 1.02$  (2%) and 1.05 (5%)). Results are shown for dry condition and DO3 as the faulty sensor.

## DISCUSSIONS

The results in this study show the performance of a simple fault detection algorithm, ARM, developed in order to detect faults in the dissolved oxygen sensor during closed loop control. The new approach is compared with AM, which monitor the aeration in every zone.

For AM the time for fault detection and isolation is the same, since this technique gets the detection and the isolation from the monitoring of one variable per faulty sensor. In the case of ARM, regarding the observed fault signature, the time instant for detection and for isolation is different. Therefore, the index definition for fault detection and isolation (based on the detection delay time and isolation time) allows comparing different monitoring techniques in terms of the number of successful detections and isolations, time for the decisions and false alarm frequency.

Table 4 shows that for the case of 1 mgO<sub>2</sub>/l of bias, similar results are obtained with AM and ARM in terms of the amount of fault detection  $FD$  and isolation  $FI$  (see also Figure 3 for 1 mgO<sub>2</sub>/l of bias). However, taking into account the instant of isolation, the index  $I_{FI}$  shows better results for ARM algorithm. This reflects that, in general, the time needed for fault isolation is lower in ARM than in the AM algorithm. The isolation time in both algorithms is similar for lower values of bias (+/- 0.25).

The sensitivity analysis for the bias given in Figure 4 shows that the ARM has a higher rate of fault detections compared to the AM algorithm, even in cases of small bias (+/-

0.25). As expected, both methods show similar performance for high level of bias ( $\pm 1$ ). However, this performance decreases when the bias is in the range of  $- 0.25$  to  $+ 0.25$ .

Concerning changes in the noise level, the results of AM and ARM given in Table 5 shows that ARM gives earlier fault detections for all the influent conditions. It can be observed in Figure 5 that, as expected, the amount of fault detections increases when the noise standard deviation is higher. Any fault detection considering a noise standard deviation equal or lower than 0.5 will be within the range of the noise in a fully functional sensor, therefore it is difficult to get a high amount of fault detections when changes in the standard deviation are around these values.

The effect of the threshold was studied for the two types of faults: bias and noise. In the case of bias fault, results in Figure 6 show that changes in the threshold do not affect the ARM performance in terms of fault detections. However, the effect of the threshold in the false alarms can be seen. ARM is more sensitive to false alarms than the AM technique, especially when the thresholds are calculated using the criteria of 2% and the bias applied is small ( $\pm 0.25$ ). Furthermore, the percentage of fault detection decreases when the level of bounds change from 2 to 5%. The index  $I_{FD}$  and  $I_{FI}$  show similar results for the two detection methods when the bias is larger than  $\pm 0.5$ . For a bias of  $\pm 0.25$  the fault detection index given by ARM is higher, it can also be seen that fault isolation of ARM in this range is lower compared to higher bias but superior if it is compared to AM.

In the case of noise faults, results in Figure 7 show that an increase in the noise standard deviation and the threshold does affect the amount of fault detections in ARM, for AM the improvement is observed more in the case of threshold of 5% than in 2%. However, the amount of fault alarms is not affected by changes in noise and threshold. The increments obtained in  $I_{FD}$  and  $I_{FI}$  give information about the reduced time achieved in fault detection and isolation, which is notorious in ARM than in AM. ARM shows a best performance in fault detection but with an inherent sensibility to false alarms, in this respect AM is less sensitive to false alarms but also less sensitive to fault detection.

Since AM and ARM are methods based on the monitoring of the manipulated variable (in this case the  $K_{La}$  value), this indirect way of monitoring makes the delay in the fault detection depend on the moment at which the fault signal occurs. For example, in the case of ARM, if there is a fault in  $DO_i$  sensor, the delay in the fault detection will be shorter if the correspondent  $f_{i,j}$  ratio is close to its maximum values. Similarly, the delay will be longer if the correspondent  $f_{i,j}$  ratio is close to its minimum values in the fault moment. The same analysis applies for the airflow monitoring in the AM algorithm.

## CONCLUSIONS

This study evaluates a new fault detection method for dissolved oxygen sensors in aerated zones. The method assumes that the DO sensors are used in closed loop control. The method can be used for an arbitrary number of zones in series. Three aerated zones are used as case study, applying the method to the BSM1. Some conclusions from the study are:

- Compared to AM, ARM gives a better performance in fault detection and isolation for noise and bias faults. But the threshold definition is more crucial in ARM than for AM, in order to have a high rank of successful fault detections and to minimize the false alarms. In this respect, a reasonable choice seems to be 5%.
- The performance of AM and ARM is decreased in the case of small bias and small change in the noise standard deviation, but even so, ARM gives a better performance in terms of false detections.
- The definition of indexes for fault detection and fault isolation allows quantifying and comparing the fault detection algorithms, taking into account not only the number of detections but the time delays involved.
- In this study we have presented a basic approach using monitoring of air flow rates (ARM). The method can be extended in several ways including:
  - By using influent water characteristics time varying bounds may be used (but this will require more instrumentation and also rely on those new sensors (for example influent ammonia sensor).
  - In practice, the airflow rate is measured with a sensor. None of the methods will be able to distinguish between faults in the DO sensor and the airflow rate sensor. An interesting alternative is to use the air valve position instead of the airflow rate.
- If there is a significant time delay in the air flows into different zones, this delay may be adjusted by calculating the ratio in Equation (3) as:

$$f_{i,j}(t) > \frac{\bar{q}_i(t)}{\bar{q}_j(t-\tau)} \quad (11)$$

where  $\tau$  is an estimate of the time delay between zone  $i$  and  $j$ . This may improve the performance of the detection. Note however that in order to calculate Equation (11) a time delay is unavoidable. An interesting topic for further research is to compare Equation (3) with (11) for systems with significant hydraulic delays.

In many plants there is a number of parallel lines, each with a number of aerated zones. A natural extension of ARM for this case is to also compute the ratios between zones in different lines.

## ACKNOWLEDGMENTS

The research leading to these results has received funding from the European Union's Seventh Framework Programme managed by REA – Research Executive Agency <http://ec.europa.eu/research/rea> (FP7/2007\_2013) under Grant Agreement N.315145 (Diamond). The MATLAB implementation of the BSM1 model has been provided by Lund University, courtesy of Ulf Jeppsson. The authors would like to thank Linda Åmand (IVL and Uppsala Universitet) and Michela Mulas (Aalto University) for their corrections and suggestions to the development of this report.

## REFERENCES

- Baggiani, F. and Marsili-Libelli, S. (2009). Real-time fault detection and isolation in biological wastewater treatment plants. *Water Science and Technology*, **60**(11), 2949–2961.
- Choi, S.W. and Lee, I-B. (2004). Nonlinear dynamic process monitoring based on dynamic kernel PCA. *Chemical Engineering Science*, **59**, 5897–5908.
- Copp, J. B. (Ed.) (2002). The COST simulation benchmark—description and simulator manual. Luxembourg: Office for Official Publications of the European Communities, ISBN 92-894-1658-0.
- Corominas, L., Villez, K., Aguado, D., Rieger, L., Rosén, C. and Vanrolleghem, P. (2011). Performance evaluation of fault detection methods for wastewater treatment processes. *Biotechnology and Bioengineering*, **108**(2), 333–344.
- Fagarasan, I. and Iliescu, S. St. (2008). Parity Equations for Fault Detection and Isolation. IEEE International Conference on Automation, Quality and Testing, Robotics, **1**, 99 – 103.
- Fragkoulis, D., Roux, G. and Dahhou B. (2011). Detection, isolation and identification of multiple actuator and sensor faults in nonlinear dynamic systems: Application to a waste water treatment process. *Applied Mathematical Modelling*, **35**, 522–543.
- Gertler, J. (1998). *Fault Detection and Diagnosis in Engineering Systems*, Marcel Dekker, New York.
- Meseguer, J., Puig, V., and Escobet, T. (2010) Fault diagnosis using a timed discrete-event approach based on interval observers: application to sewer networks. *IEEE Transactions on Systems, Man and Cybernetics – Part A: Systems and Humans*, **40**(5), 900–916.
- Ragot, J. and Maquin, D. (2006). Fault measurement detection in an urban water supply network. *Journal of Process Control*, **16**, 887–902.
- Rieger, L., Alex, J., Winkler, S., Boehler, M., Thomann, M. and Siegrist, H. (2003) Progress in sensor technology – progress in process control? Part I: Sensor property investigation and classification. *Water Science and Technology*, **47**(2), 103–112.
- Rosen, C. and Lennox, J.A. (2001). Multivariate and multiscale monitoring of wastewater treatment operation. *Water Research*, **35**(14), 3402–3410.
- Rosen, C., Rieger, L., Jeppson, U. and Vanrolleghem, P. (2008). Adding realism to simulated sensors and actuators. *Water Science and Technology*, **57**(3), 337–344.
- Steyer, J-Ph., Genovesi, A. and Harmand, J. (2001). Advanced monitoring and control of anaerobic wastewater treatment plants: fault detection and isolation. *Water Science and Technology*, **43**(7), 183–190.